Journal of Earth Science, *Vol. 20*, *No. 2*, *p. 241–249*, *April 2009* *ISSN 1674-487X*
Printed in China
DOI: 10.1007/s00000-001-0023-1

Mantle Input to the Crust in Southern Gangdese, Tibet, during the Cenozoic: Zircon Hf Isotopic Evidence

Mo Xuanxue* (莫宣学), **Dong Guochen** (董国臣), **Zhao Zhidan** (赵志丹),
Zhu Dicheng (朱弟成), **Zhou Su** (周肃)
State Key Laboratory of Geological Processes and Mineral Resources, *School of the Earth Sciences and Resources*, *China University of Geosciences*, *Beijing* 100083, *China*
Yaoling Niu
Department of Earth Sciences, *Durham University*, *Durham DH*1 3*LE*, *UK*

ABSTRACT: The Quxu (曲水) complex is a typical intrusive among the Gangdese batholiths. Two sets of samples collected from the Mianjiang (棉将) and Niedang (聂当) villages in Quxu County, including gabbro, mafic micro-enclaves (MME), and granodiorites in each set, were well dated in a previous SHRIMP zircon U-Pb analysis (47–51 Ma). In this article, the same zircons of the 6 samples were applied for LA ICP-MS Hf isotopic analysis. The total of 6 samples yields $^{176}Hf/^{177}Hf$ ratio ranging from 0.282 921 to 0.283 159, corresponding to $\varepsilon_{Hf}(t)$ values of 6.3–14.7. Their Hf depleted-mantle modal ages (T_{DM}) are in the range of 137–555 Ma, and the zircon Hf isotope crustal model ages (T_{DM}^{C}) range from 178 to 718 Ma. The mantle-like high and positive $\varepsilon_{Hf}(t)$ values in these samples suggest a mantle-dominated input of the juvenile source regions from which the batholith originated. The large variations in $\varepsilon_{Hf}(t)$ values, up to 5-ε unit among zircons within a single rock and up to 15-ε unit among zircons from the 6 samples, further suggest the presence of a magma mixing event during the time of magma generation. We suggest that the crustal end-member involved in the magma mixing is likely from the ancient basement within the Lhasa terrane itself. The zircon Hf isotopic compositions further suggest that magma mixing and magma underplating at about 50 Ma may have played an important role in creating the crust of the southern Tibetan plateau.

KEY WORDS: Tibetan plateau, Gangdese batholith, Quxu complex, gabbro, MME, granodiorite, zircon Hf isotope, magma mixing, crustal thickening.

INTRODUCTION

The Gangdese batholith in the southern margin of the Lhasa terrane, which is one of the largest intrusive belts on earth, extending over 2 000 km east-west along the India-Yarlung Zangbo suture zone, is generally accepted as the product of the Tethyan oceanic subduction and subsequent India-Asia continental collision. The magmatism started as early as the Late Triassic, and ceased at ~10 Ma, recording long-lasting crust-mantle interaction processes and therefore pro-

This study was supported by the National Basic Research Program of China (Nos. 2009CB421002, 2002CB412600), the National Natural Science Foundation of China (Nos. 40873023, 40830317, 40672044, 40503005, 40572048, 40473020), 111 Project (No. B07011), China Geological Survey (No. 1212010610104).

*Corresponding author: moxx@cugb.edu.cn

Manuscript received November 25, 2008.
Manuscript accepted January 28, 2009.

viding an important opportunity for exploring the timing and style of the crustal growth of the Asian continent (Ji et al., 2009; Mo et al., 2008, 2007, 2005a, b; Wen et al., 2008; Chu et al., 2006; Chung et al., 2005, 2003; Dong et al., 2005; Hou et al., 2004).

Based on our previous detailed field geological mapping and SHRIMP zircon U-Pb dating on part of the Quxu granitoid complex close to Lhasa, abundant mafic micro-enclaves (MME) and gabbros are recognized within the host granitoid and are involved as the mafic end-member during the magma mixing events that peaked at ~50 Ma (Dong et al., 2005; Mo et al., 2005a). Such peak magmatism at ~50 Ma was recently confirmed by 25 SHRIMP zircon U-Pb ages sampled along ~800 km length of the Gangdese batholiths (including gabbro, gabbroic enclave, diorite, granodiorite, and granite) from Dajia Co in the west to Bomi in the east (Wen et al., 2008). These authors referred to this peak magmatism as the magmatic "flare-up" event and attributed it to the slab breakoff of the subducted Neo-Tethyan oceanic lithosphere. Unfortunately, no isotopic data are available in Wen et al. (2008) that could further address the mantle origin of the complex. A more recent work by Ji et al. (2009) revealed a systematic dataset of LA ICP-MS zircon U-Pb ages and Hf isotopic compositions on the Gangdese batholiths in southern Tibet, revealing that the magmatism occurred from 205 to 13 Ma, and can be compared with the Kohistan-Ladakh batholiths in the west and the Chayu-Burma batholiths in the east. They also pointed out that the third stage of 65–41 Ma, which had the most juvenile nature among the four divisions, is the most prominent period of granitic magmatism in the Gangdese batholith. These new zircon Hf isotopic data substantially support the previous recognition that the Gangdese batholiths are distinctly characterized by positive $\varepsilon_{Nd}(t)$ values (Jiang et al., 1999; Harris et al., 1988). Such prominent granitoid magmatism, in combination with the contemporaneous Linzizong volcanic successions (65–41 Ma, Lee et al., 2007; Zhou et al., 2004) that are also characterized by mantle-like positive $\varepsilon_{Nd}(t)$ values, suggests a significant mantle contribution to the crust, which therefore played a significant role in creating the thickened crust beneath the Tibetan plateau (Mo et al., 2008, 2007).

In this article, based on our previously published SHRIMP zircon U-Pb ages of the granitoids and related mafic rocks in the Quxu batholith, we present our newly obtained zircon Hf isotopic data on the same samples. We, (1) discovered an extensive mantle input when magmatism peaked at ~50 Ma, (2) discuss the contribution of this huge flux from the mantle to the crust, and (3) consider it as an important mechanism in thickening the crust during the early stage of the India-Asia continental collision.

GEOLOGICAL SETTING AND SAMPLES

The Quxu pluton is one of the typical plutons among the Gangdese batholiths that have attracted many studies both in dating and geochemistry since the Sino-France and Sino-British collaborations in the 1980s. A detailed field mapping on this pluton (Dong et al., 2005; Mo et al., 2005a, b) revealed that the granitoids and related mafic bodies and MME were emplaced almost synchronously, ranging from 45 to 55 Ma, with a peak emplacement age of ~50 Ma. The elemental and Sr-Nd-Pb isotopic investigation on rocks, from gabbros to granites, in the Quxu complex led to the recognition of a magma mixing event and an associated magma underplating process (Dong et al., 2008, 2006, 2005; Mo et al., 2005a).

Six samples previously dated by SHRIMP zircon U-Pb dating (Mo et al., 2005a) were selected for zircon Hf isotopic analysis. These six samples were collected from two localities: the first set (samples SZ0345-A, B, D) from Mianjiang Village (29°21.7'N, 90°42.5'E) in the southern Quxu pluton and the second set (samples SQ0343-A, B, C) from Niedang Village (29°29.9'N, 90°56.3'E) in the northern Quxu pluton. The age and lithology of these six samples are listed in Table 1. The ages range from 47 to 51 Ma, with a peak age of ~50 Ma. The dating results (Mo et al., 2005a) and geochemical modeling (Dong et al., 2006) suggest that the rocks (including gabbro, MME, and granodiorite) are all mantle origin and/or mantle-input-related, and members of magma mixing processes.

ANALYTICAL METHODS

Zircon Hf isotope analysis was done on the same dated spots using LA ICP-MS with a beam size of 60 μm and a laser pulse frequency of 8 Hz at the Insti-

Table 1 Summary of zircon Hf isotopic results of the gabbro-granite rock in the Gangdese botholiths, southern Tibet

Sample	Lithology	Age (Ma)	SiO_2 (wt.%)	$\varepsilon_{Hf}(0)$	$\varepsilon_{Hf}(t)$	T_{DM} (Ma)	T_{DM}^C (Ma)	$\varepsilon_{Nd}(t)$
SQ0345A	MME	49.9±1.7	54.49	10.7 (9.6 –12.2)	11.8 (10.6–13.2)	250 (189–293)	369 (273–442)	5.55
SQ0345B	Gabbro	48.9±1.1	52.42	8.9 (5.5–10.5)	10.0 (6.3–11.7)	338 (258–555)	485 (379–718)	
SQ0345C	Diorite	49.3±1.7	57.07	11.2 (10.1–12.4)	12.2 (11.2–13.4)	232 (183–276)	341 (264–409)	
SZ0343A	Granodiorite	51.2±1.1	63.03	9.1 (8.2–10.1)	10.2 (9.4–11.2)	316 (276–350)	474 (410–528)	
SZ0343B	Am-gabbro	47.0±1.0	50.26	10.0 (8.5–13.8)	11.0 (9.3–14.7)	293 (137–370)	419 (178–522)	3.97
SZ0343D	MME	51.1±1.1	47.43	8.8 (7.7–10.0)	9.8 (8.7–11.0)	335 (282–383)	495 (419–567)	

Note: the ages are SHRIMP zircon $^{206}Pb/^{238}U$ results from Mo et al. (2005a). Data in the parentheses represent the data range of $\varepsilon_{Hf}(0)$, $\varepsilon_{Hf}(t)$, T_{DM} (Ma), and T_{DM}^C (Ma) that are listed in Table 2. Whole rock SiO_2 compositions and $\varepsilon_{Nd}(t)$ are from Dong et al. (2006).

tute of Geology and Geophysics, Chinese Academy of Sciences, Beijing. The details of the instrumental conditions and data acquisition are given in Wu et al. (2006) and Ji et al. (2009). During analysis, the $^{176}Hf/^{177}Hf$ and $^{176}Lu/^{177}Hf$ ratios of the standard zircon (91500) were 0.282 322±22 ($2\sigma_n$, n=28) and 0.000 319, consistent with the values (0.282 307±31, $2\sigma_n$, n=44) obtained previously in this laboratory (Wu et al., 2006).

ZIRCON Lu-Hf ISOTOPIC RESULTS

A total of 90 sets of $^{176}Hf/^{177}Hf$ isotopic data on the zircons from the 6 samples are listed in Table 2. A summary of the results is given in Table 1. The results are also plotted in $\varepsilon_{Hf}(t)$ against their ages in Fig. 1. The $\varepsilon_{Hf}(t)$ values (the parts in 10^4 deviation of the initial Hf isotope ratios between the zircon sample and the chondritic reservoir) and T_{DM}^C (the zircon Hf isotope crustal model ages based on a depleted-mantle source and an assumption that the protolith of the zircon's host magma has an average continental crustal $^{176}Lu/^{177}Hf$ ratio of 0.015) were calculated following Griffin et al. (2002) using the ^{176}Lu decay constant adopted in Blichert-Toft and Albarède (1997).

In the three samples (SZ0345-A, B, D) of the first set that was collected in Mianjiang Village, the U-Pb ages range from 48.9 to 49.9 Ma (Mo et al., 2005a); the $^{176}Hf/^{177}Hf$ ratio ranges from 0.283 045 to 0.283 118 ($\varepsilon_{Hf}(t)$=10.6–13.2) in the gabbroid MME sample (SQ0345A), from 0.282 928 to 0.283 070 ($\varepsilon_{Hf}(t)$=6.3–11.7) in the gabbro sample (SQ0345B), and from 0.283 058 to 0.283 123 ($\varepsilon_{Hf}(t)$=11.2–13.4) in the diorite sample (SQ0345C) (Tables 1 and 2, Fig. 1a). Their $\varepsilon_{Hf}(t)$ values decrease slightly with decreasing SiO_2 content (Fig. 1b). The positive $\varepsilon_{Hf}(t)$ values in these samples are consistent with a mantle origin of the gabbros and mantle-input-related diorite. The zircon Hf isotope model ages based on a depleted-mantle source (T_{DM}) are in the range of 230–338 Ma.

In the three samples of the second set that was collected in Niedang Village (47–51 Ma, Mo et al., 2005a), the $^{176}Hf/^{177}Hf$ ratios and $\varepsilon_{Hf}(t)$ values of the amphibole gabbro (SZ0343B, 0.283 012–0.283 163, $\varepsilon_{Hf}(t)$=9.3–14.7) are slightly greater than those of the granodiorite (SZ0343A, 0.283 005–0.283 057, $\varepsilon_{Hf}(t)$= 9.4–11.2) and the gabbroidic MME (SZ0343D, 0.282 990–0.283 054, $\varepsilon_{Hf}(t)$=8.7–11.0). The T_{DM} values of the three samples range from 293 to 335 Ma. These samples also show depleted-mantle Hf isotopic features. As a whole, the gabbros show a decreasing trend in $\varepsilon_{Hf}(t)$ value with decreasing SiO_2 content (Fig. 1b).

DISCUSSION

Extensive Mantle Input during India-Asia Collision

The zircon Hf isotopic data of the six samples of the Quxu pluton from Mianjiang and Niedang reported in this study further support this point. The average $\varepsilon_{Hf}(t)$ values of the samples, including gabbros, gabbroic MMEs, and granodiorites, range from 10 to 12.2 (Table 2). The variation within one sample can be as high as 5.4 units of $\varepsilon_{Hf}(t)$ (such as that in two gabbros, SQ0345B and SZ0343B). They have a young

Table 2 Zircon Hf isotopic results of the gabbro-granite rock in the Gangdese batholiths, southern Tibet

No.	Age (Ma)	$^{176}Yb/^{177}Hf$	$^{176}Lu/^{177}Hf$	$^{176}Hf/^{177}Hf$	2σ	$^{176}Hf/^{177}Hf_i$	$\varepsilon_{Hf}(0)$	$\varepsilon_{Hf}(t)$	T_{DM} (Ma)	T_{DMC} (Ma)	$f_{Lu/Hf}$
SQ0345A, MME, 49.9±1.7 Ma											
02	51	0.026 700	0.001 076	0.283 080	0.000 020	0.283 079	10.9	12.0	244	359	-0.97
03	50	0.027 398	0.001 110	0.283 065	0.000 018	0.283 064	10.4	11.4	265	392	-0.97
04-1	47	0.023 596	0.000 943	0.283 078	0.000 018	0.283 077	10.8	11.8	246	366	-0.97
04	47	0.024 831	0.000 990	0.283 118	0.000 017	0.283 117	12.2	13.2	189	273	-0.97
05	49	0.027 611	0.001 109	0.283 090	0.000 017	0.283 089	11.2	12.3	229	336	-0.97
06	55	0.033 832	0.001 350	0.283 096	0.000 018	0.283 095	11.5	12.6	222	320	-0.96
07	51	0.013 854	0.000 571	0.283 093	0.000 016	0.283 093	11.4	12.5	221	326	-0.98
08	49	0.026 523	0.001 047	0.283 080	0.000 016	0.283 079	10.9	11.9	243	359	-0.97
09	53	0.026 990	0.001 067	0.283 079	0.000 019	0.283 078	10.9	12.0	245	359	-0.97
10	48	0.025 315	0.001 000	0.283 055	0.000 019	0.283 054	10.0	11.0	279	417	-0.97
11	49	0.021 272	0.000 850	0.283 062	0.000 018	0.283 061	10.3	11.3	268	400	-0.97
12	50	0.026 263	0.001 057	0.283 049	0.000 019	0.283 048	9.8	10.9	288	429	-0.97
13	55	0.026 712	0.001 079	0.283 051	0.000 020	0.283 050	9.9	11.0	285	422	-0.97
14	59	0.028 626	0.001 138	0.283 071	0.000 021	0.283 069	10.6	11.8	257	375	-0.97
15	45	0.024 211	0.000 958	0.283 045	0.000 019	0.283 044	9.6	10.6	293	442	-0.97
16	49	0.027 142	0.001 069	0.283 079	0.000 019	0.283 078	10.8	11.9	245	362	-0.97
17	45	0.024 981	0.000 997	0.283 092	0.000 017	0.283 091	11.3	12.3	226	335	-0.97
SQ0345B, gabbro, 48.9±1.1 Ma											
01-0	48	0.020 371	0.000 904	0.283 001	0.000 036	0.283 001	8.1	9.1	354	538	-0.97
01	48	0.038 318	0.001 521	0.283 035	0.000 024	0.283 033	9.3	10.3	312	464	-0.95
06	47	0.203 673	0.007 456	0.282 928	0.000 034	0.282 921	5.5	6.3	555	718	-0.78
09	57	0.025 815	0.001 037	0.283 051	0.000 029	0.283 050	9.9	11.1	284	420	-0.97
12	48	0.030 514	0.001 316	0.283 065	0.000 023	0.283 064	10.4	11.4	266	394	-0.96
13	55	0.024 513	0.001 122	0.283 070	0.000 025	0.283 069	10.5	11.7	258	379	-0.97
SQ0345C, diorite, 49.3±1.7 Ma											
01	50	0.025 374	0.001 032	0.283 095	0.000 019	0.283 094	11.4	12.5	222	325	-0.97
02	52	0.020 172	0.000 821	0.283 081	0.000 017	0.283 080	10.9	12.0	240	354	-0.98
03	56	0.020 280	0.000 811	0.283 112	0.000 015	0.283 111	12.0	13.2	197	282	-0.98
04	49	0.022 204	0.000 897	0.283 079	0.000 017	0.283 078	10.9	11.9	243	361	-0.97
05-1	46	0.016 538	0.000 683	0.283 085	0.000 015	0.283 084	11.1	12.0	234	349	-0.98
05	46	0.031 018	0.001 250	0.283 123	0.000 017	0.283 121	12.4	13.4	183	264	-0.96
07	44	0.018 991	0.000 790	0.283 069	0.000 017	0.283 069	10.5	11.5	257	386	-0.98
08-1	52	0.014 511	0.000 607	0.283 093	0.000 015	0.283 093	11.4	12.5	222	326	-0.98
08	52	0.027 222	0.001 098	0.283 108	0.000 016	0.283 107	11.9	13.0	203	293	-0.97
09	50	0.028 401	0.001 122	0.283 066	0.000 019	0.283 065	10.4	11.5	264	391	-0.97
10	52	0.020 193	0.000 833	0.283 104	0.000 016	0.283 103	11.7	12.9	207	302	-0.97
11	50	0.034 169	0.001 344	0.283 084	0.000 020	0.283 083	11.0	12.1	239	350	-0.96
12-1	52	0.022 308	0.000 891	0.283 075	0.000 021	0.283 074	10.7	11.8	249	368	-0.97
13-1	50	0.013 768	0.000 577	0.283 080	0.000 021	0.283 080	10.9	12.0	240	356	-0.98
13	50	0.028 714	0.001 170	0.283 058	0.000 022	0.283 057	10.1	11.2	276	409	-0.96
SZ0343A, granodiorite, 51.2±1.1 Ma											
01-1	50	0.028 175	0.001 216	0.283 031	0.000 015	0.283 030	9.2	10.2	314	470	-0.96
01	50	0.031 099	0.001 364	0.283 009	0.000 018	0.283 008	8.4	9.4	347	520	-0.96
02-1	50	0.025 980	0.001 135	0.283 028	0.000 017	0.283 027	9.1	10.1	318	477	-0.97
02-2	50	0.030 507	0.001 249	0.283 049	0.000 014	0.283 048	9.8	10.8	289	430	-0.96

Continued

No.	Age (Ma)	$^{176}Yb/^{177}Hf$	$^{176}Lu/^{177}Hf$	$^{176}Hf/^{177}Hf$	2σ	$^{176}Hf/^{177}Hf_i$	$\varepsilon_{Hf}(0)$	$\varepsilon_{Hf}(t)$	T_{DM} (Ma)	T_{DMC} (Ma)	$f_{Lu/Hf}$
02	50	0.026 839	0.001 126	0.283 008	0.000 016	0.283 007	8.4	9.4	346	522	-0.97
03	51	0.018 809	0.000 799	0.283 027	0.000 017	0.283 026	9.0	10.1	317	478	-0.98
04	54	0.020 390	0.000 867	0.283 030	0.000 015	0.283 029	9.1	10.3	313	469	-0.97
05	49	0.020 929	0.000 913	0.283 040	0.000 017	0.283 039	9.5	10.5	299	449	-0.97
06	49	0.021 330	0.000 927	0.283 035	0.000 017	0.283 034	9.3	10.4	306	461	-0.97
07	50	0.019 990	0.000 867	0.283 045	0.000 016	0.283 044	9.7	10.7	292	438	-0.97
08	51	0.019 335	0.000 833	0.283 023	0.000 016	0.283 022	8.9	10.0	322	487	-0.97
09-1	54	0.029 083	0.001 245	0.283 012	0.000 015	0.283 011	8.5	9.6	342	511	-0.96
09	54	0.017 926	0.000 813	0.283 036	0.000 016	0.283 035	9.3	10.5	305	457	-0.98
10	53	0.025 252	0.001 043	0.283 005	0.000 015	0.283 004	8.2	9.4	350	528	-0.97
11-1	52	0.027 122	0.001 235	0.283 024	0.000 018	0.283 023	8.9	10.0	325	485	-0.96
11	52	0.018 895	0.000 839	0.283 010	0.000 017	0.283 009	8.4	9.5	341	517	-0.97
12-1	54	0.019 370	0.000 864	0.283 056	0.000 016	0.283 055	10.1	11.2	276	410	-0.97
12	54	0.020 117	0.000 855	0.283 027	0.000 016	0.283 026	9.0	10.2	317	476	-0.97
13-1	51	0.032 834	0.001 421	0.283 057	0.000 015	0.283 055	10.1	11.1	279	411	-0.96
13	51	0.020 719	0.000 873	0.283 026	0.000 015	0.283 025	9.0	10.1	319	481	-0.97
SZ0343B, Am-gabbro, 47.0±1.0 Ma											
01-1	48	0.095 181	0.004 206	0.283 040	0.000 028	0.283 036	9.5	10.4	328	457	-0.87
01	48	0.101 174	0.004 477	0.283 163	0.000 020	0.283 159	13.8	14.7	137	178	-0.87
02	47	0.062 245	0.002 588	0.283 060	0.000 019	0.283 058	10.2	11.1	284	409	-0.92
03	50	0.052 348	0.002 265	0.283 031	0.000 020	0.283 029	9.2	10.2	324	473	-0.93
04	49	0.020 630	0.000 904	0.283 076	0.000 020	0.283 075	10.8	11.8	248	368	-0.97
05	48	0.022 448	0.000 964	0.283 082	0.000 022	0.283 081	11.0	12.0	240	355	-0.97
06	45	0.046 412	0.001 903	0.283 050	0.000 019	0.283 049	9.8	10.8	292	431	-0.94
07	46	0.164 186	0.006 343	0.283 061	0.000 025	0.283 056	10.2	11.1	314	413	-0.81
08	48	0.141 090	0.005 865	0.283 030	0.000 025	0.283 025	9.1	10.0	360	482	-0.82
09	46	0.060 703	0.002 504	0.283 050	0.000 022	0.283 048	9.8	10.8	298	432	-0.92
10	45	0.077 124	0.003 167	0.283 087	0.000 028	0.283 084	11.1	12.0	248	350	-0.90
11	50	0.024 713	0.001 114	0.283 021	0.000 021	0.283 020	8.8	9.9	328	493	-0.97
12	47	0.052 130	0.002 431	0.283 032	0.000 028	0.283 030	9.2	10.2	324	472	-0.93
13	47	0.053 461	0.002 252	0.283 078	0.000 024	0.283 076	10.8	11.8	254	367	-0.93
14	45	0.088 266	0.004 074	0.283 012	0.000 027	0.283 008	8.5	9.3	370	522	-0.88
15	47	0.058 327	0.002 574	0.283 020	0.000 023	0.283 018	8.8	9.7	342	499	-0.92
SZ0343D, MME, 51.1±1.1 Ma											
01-1	51	0.100 233	0.004 136	0.283 008	0.000 031	0.283 004	8.3	9.3	377	529	-0.88
01-2	51	0.059 545	0.002 520	0.283 054	0.000 024	0.283 052	10.0	11.0	291	419	-0.92
01	51	0.074 020	0.002 998	0.282 998	0.000 022	0.282 995	8.0	9.0	380	549	-0.91
02-1	53	0.033 822	0.001 485	0.283 049	0.000 018	0.283 048	9.8	10.9	291	428	-0.96
02	53	0.024 348	0.001 036	0.283 027	0.000 019	0.283 026	9.0	10.1	319	478	-0.97
03-1	49	0.027 663	0.001 184	0.283 028	0.000 019	0.283 027	9.0	10.1	319	478	-0.96
03	49	0.022 080	0.000 961	0.283 004	0.000 017	0.283 003	8.2	9.2	351	533	-0.97
04	50	0.027 256	0.001 195	0.283 024	0.000 019	0.283 023	8.9	10.0	324	486	-0.96
05	52	0.023 368	0.001 036	0.283 053	0.000 020	0.283 052	9.9	11.0	282	419	-0.97
06-1	46	0.051 745	0.002 109	0.282 990	0.000 018	0.282 988	7.7	8.7	382	567	-0.94
06	46	0.019 339	0.000 838	0.283 012	0.000 020	0.283 012	8.5	9.5	338	514	-0.97

Continued

No.	Age (Ma)	$^{176}Yb/^{177}Hf$	$^{176}Lu/^{177}Hf$	$^{176}Hf/^{177}Hf$	2σ	$^{176}Hf/^{177}Hf_i$	$\varepsilon_{Hf}(0)$	$\varepsilon_{Hf}(t)$	T_{DM} (Ma)	T_{DMC} (Ma)	$f_{Lu/Hf}$
07	48	0.030 991	0.001 361	0.283 042	0.000 020	0.283 041	9.5	10.6	300	447	-0.96
08	46	0.070 936	0.003 045	0.282 996	0.000 022	0.282 994	7.9	8.8	383	555	-0.91
09	51	0.030 491	0.001 302	0.283 005	0.000 022	0.283 004	8.2	9.3	352	529	-0.96
10	50	0.030 531	0.001 258	0.283 013	0.000 018	0.283 012	8.5	9.6	341	512	-0.96
11	55	0.051 808	0.002 164	0.283 025	0.000 021	0.283 023	8.9	10.1	332	484	-0.93

Note: the ages are SHRIMP zircon U-Pb $^{206}Pb/^{238}U$ ages (Mo et al., 2005a).

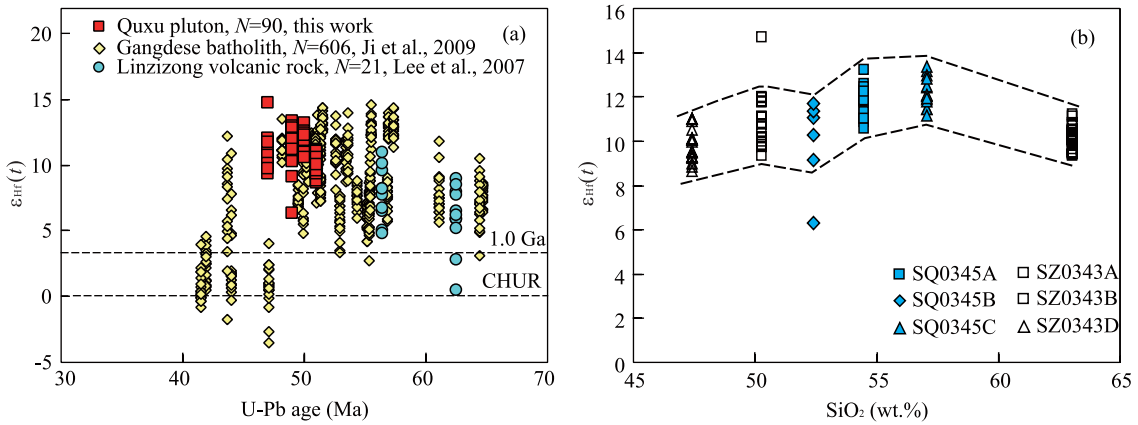

Figure 1. Plots of $\varepsilon_{Hf}(t)$ vs. ages (a) and whole-rock SiO_2 content (b) of the Quxu gabbro-granitoid complex in southern Tibet. Sources of age data are the same as in Tables 1 and 2.

Hf model age (230–340 Ma). These depleted mantle-like high and positive $\varepsilon_{Hf}(t)$ values suggest that the Quxu complex, one of the typical Gangdese batholiths, is generated from either the mantle wedge or a pre-existing mafic lower crust beneath the collision zone instead of the general granites that originated from the recycling of a sedimentary lower continental crust. The majority of a widely sampled research also shows this positive and wide range variation in $\varepsilon_{Hf}(t)$ values, with the $\varepsilon_{Hf}(t)$ values changing from 4 to 15, corresponding to the ages between 47 and 70 Ma, and the T_{DM}(Hf) from 510 to 730 Ma (Ji et al., 2009). These zircon Hf isotopic signatures are consistent with the Nd isotopic compositions ($\varepsilon_{Nd}(t)$=2–8.5, DePaolo et al., 2008; Dong et al., 2008; Jiang et al., 1999; Harris et al., 1988).

The Paleogene Linzizong volcanic succession that was studied in detail in the Linzhou basin (LVS, 40–65 Ma) temporally overlaps with the Gangdese batholiths. It is similarly regarded as a product of Tethyan subduction-related magmatism and also shows mantle-like Nd-Sr features (Mo et al., 2008, 2007, 2005a, b, 2003; Zhou et al., 2004). The zircon Hf isotope of LVS reported by Lee et al. (2007) (Fig. 1) is also the same as that of the Gangdese batholiths.

The Hf isotope results obtained in this study and others (Ji et al., 2009; Lee et al., 2007) in the central Gangdese batholith and related volcanic rocks further support that the mantle materials were added to the crust via the partial melting of the subducted remaining part of the Tethyan Ocean crust (Mo et al., 2008) or the recycling of the pre-existing oceanic arc terrane (with positive $\varepsilon_{Nd}(t)$ values) (Ji et al., 2009). This is an important issue in figuring out whether the collisional zone is also the place of crustal growth from below (Mo et al., 2008).

To the west syntaxis, the western extension of the Gangdese batholith in Ladakh and Karakoram, the same situation was also found by Ravikant et al. (2009). The granite and diorite from the Ladakh batholith (50–68 Ma) have $\varepsilon_{Hf}(t)$ values ranging from 7.4 to 10.3, corresponding to a young model age (T_{DM}(Hf)=510–730 Ma). Therefore, such a significant feature (high and positive $\varepsilon_{Hf}(t)$ values and a young Hf

model age) in a large spatial frame from Ladakh to the Gangdese batholith suggests a giant mantle-to-crust process through the magmatism during the early collision between India and Asia (Ji et al., 2009).

Constraints in Magma Mixing

Magma mixing processes were employed in describing the petrogenesis of the Quxu pluton, and the portions of basic and acid end-members involved in the mixing event were quantitatively estimated using major elemental compositions (Dong et al., 2008, 2006, 2005; Mo et al., 2007, 2005a, b). The remaining issue is that the two proposed end-members cannot be recognized by Nd-Sr-Pb isotopes in terms of the most mafic portion having the highest Nd and the least Sr isotopic ratios. For instance, the $\varepsilon_{Nd}(t)$ values changed from 2.7 to 8.5, unrelated to their SiO_2 contents (47 wt.%–56 wt.%) (Dong et al., 2008). This is explained as one of the geochemical features for supporting a magma mixing origin of granite and related rocks, indicating that the magma has been chemically homogeneous during the mixing processes (Dong et al., 2008, 2006; Mo et al. 2005a, b).

In the Hf results of this work (Fig. 1b), there are no correlations between the $\varepsilon_{Hf}(t)$ values and their SiO_2 contents. For example, the most basic sample (SZ0343D) has the lowest mean $\varepsilon_{Hf}(t)$ values (8.8) among all the 6 samples, even lower than that of the granodiorite (9.1 in sample SZ0343A). This is similar to the above-mentioned Nd-Sr isotopes. In this point, the zircon Hf isotopic results are consistent with the Nd-Sr data. This was also discovered by Ji et al. (2009), who pointed out that no significant Hf isotopic difference existed between the mantle-derived gabbro and the crustal-derived granite, further indicating that these zircons were crystallized from different kinds of host magmas.

However, it should be noted that there are large variations in zircon $\varepsilon_{Hf}(t)$ values, up to 5.4-ε units within a single rock and up to 15-ε units between zircons within the six contemporaneous samples of ~50 Ma. Similar large variations in the zircon Hf isotopic compositions of the Quxu pluton are also observed in the granitoids (133–117 Ma) in eastern Tibet (Chiu et al., 2009), the Fogang batholith in SE China (Li et al., 2007), the granitoids in the Lachlan fold belt of Australia, and the separation point suite of New Zealand (Bolhar et al., 2008; Kemp et al., 2007). This heterogeneity requires an open system with more than 2 end-member mixtures of the magma source region instead of partial melting or fractional crystallization. In other words, the large variations in zircon $\varepsilon_{Hf}(t)$ values observed in the Quxu pluton are indicative of magma mixing.

Then, the remaining issue is which "crust" end-member was involved during the magma mixing in the Gangdese batholiths. In Fig. 1a, there is no zircon with crustal signature ($\varepsilon_{Hf}(t)<0$) with an age range of ~65–47 Ma, suggesting that the majority of the source region are mantle-like materials or even a small number of crustal input. But at ~47 Ma, the crustal components with negative $\varepsilon_{Hf}(t)$ values appeared. Such a change was interpreted by Ji et al. (2009) as the involvement of old crustal material and was attributed to the input of Indian continental crust materials. But a just finished article by Zhu et al. (2009) reported that the Paleocene diorite (~62 Ma) south of Nanmulin contains a large amount of inherited Proterozoic zircon (466–1 632 Ma) with $\varepsilon_{Hf}(t)$ values ranging from -9.9 to 4.6 (T_{DM}^{C}=1.46–2.53 Ga). The emplacement age of the diorite significantly predates by about 10 Ma the arrival of the Indian continental crust beneath the Gangdese batholith (Chung et al., 2005). Therefore, the finding would indicate that the crustal materials involved in the magma mixing of the Gangdese batholith may have come from the Lhasa terrane itself rather than the Indian continent.

Constraints in the Crust Thickening and Growth on Tibetan Plateau

In a recent study, Mo et al. (2007) divided the postcollisional process into three phases after the India-Asia collision around 65–70 Ma based on a systematic research on the associated magmatism. They discussed the contributions of the magmatism to the crustal thickening during each phase. Among the three, Phase I, which is represented by the syn- collisional LVS volcanism (~65–40 Ma) and the emplacement of southern Gangdese batholiths (a peak age of ~50 Ma), is the key period for the formation of the lower juvenile crust via the input of mantle-derived magmas and caused the crustal thickening in southern Tibet. The

authors proposed that the mantle material input contributed about 30% (about 20 km) to the total thickness of the present-day Tibetan crust. The zircon Hf isotopic compositions reported in this study, in combination with the data recently published (Ji et al., 2009; Lee et al., 2007), further confirmed this mantle input to the crust of southern Tibet. In this regard, the zircon Hf isotopic compositions provide new insights to justify the previous interpretation (Mo et al., 2007) that the magma mixing and magma underplating at about 50 Ma may have played an important role in creating the crust of the southern Tibetan plateau.

CONCLUSIONS

(1) Six samples (including gabbro, mafic microenclaves (MME), and granodiorites) used for LA ICP-MS zircon Hf isotopic analysis of the Quxu complex yielded $^{176}Hf/^{177}Hf$ ratios ranging from 0.282 921 to 0.283 159, corresponding to $\varepsilon_{Hf}(t)$ values of 6.3 to 14.7. Their T_{DM} and T_{DM}^{C} are in the range of 137 to 555 Ma and 178 to 718 Ma, respectively.

(2) The mantle-like high and positive $\varepsilon_{Hf}(t)$ values of the samples suggest a mantle input of the juvenile source regions.

(3) There is no relationship between the sample composition and the $^{176}Hf/^{177}Hf$ compositions. A large variation in $\varepsilon_{Hf}(t)$ values within a single rock (up to 5.4-ε units) and within the 6 samples (up to 15-ε units) is observed. These further suggest that the magma mixing and magma underplating at about 50 Ma may have played an important role in creating the crust of the southern Tibetan plateau.

ACKNOWLEDGMENT

This study was supported by the National Basic Research Program of China (Nos. 2009CB421002, 2002CB412600), the National Natural Science Foundation of China (Nos. 40873023, 40830317, 40672044, 40503005, 40572048, 40473020), 111 Project (No. B07011), China Geological Survey (No. 1212010610104). Prof. Yang Jingsui is thanked for his warmly inviting to write this article. We thank Wu Fuyuan, Xie Liewen, Yang Yueheng and Sun Jinfeng for the help during the Hf analysis in IGGCAS.

REFERENCES CITED

Blichert-Toft, J., Albarede, F., 1997. The Lu-Hf Isotope Geochemistry of Chondrites and the Evolution of the Mantle-Crust System. *Earth Planet. Sci. Lett*., 148: 243–258

Bolhar, R., Weaver, S. D., Whitehouse, M. J., et al., 2008. Sources and Evolution of Arc Magmas Inferred from Coupled O and Hf Isotope Systematics of Plutonic Zircons from the Cretaceous Separation Point Suite (New Zealand). *Earth Planet. Sci. Lett*., 268(3–4): 312–324

Chiu, H. Y., Chung, S. L., Wu, F. Y., et al., 2009. Zircon U-Pb and Hf Isotope Constraints from Eastern Transhimalayan Batholiths on the Precollisional Magmatic and Tectonic Evolution in Southern Tibet. *Tectonophysics* (Submitted)

Chu, M. F., Chung, S. L., Song, B., et al., 2006. Zircon U-Pb and Hf Isotope Constraints on the Mesozoic Tectonics and Crustal Evolution of Southern Tibet. *Geology*, 34(9): 745–748

Chung, S. L., Chu, M. F., Zhang, Y. Q., et al., 2005. Tibetan Tectonic Evolution Inferred from Spatial and Temporal Variations in Post-Collisional Magmatism. *Earth-Science Reviews*, 68(3–4): 173–196

Chung, S. L., Liu, D. Y., Ji, J. Q., et al., 2003. Adakites from Continental Collision Zones: Melting of Thickened Lower Crust beneath Southern Tibet. *Geology*, 31(11): 1021–1024

DePaolo, D. J., Weaver, K. L., Mo, X. X., et al., 2008. Regional Isotopic Patterns in Granitic Rocks of Southern Tibet and Evolution of Crustal Structure during the Indo-Asian Collision. *Geochimica et Cosmochimica Acta*, 72(12, Suppl.): A211

Dong, G. C., Mo, X. X., Zhao, Z. D., et al., 2005. Geochronologic Constraints on the Magmatic Underplating of the Gangdise Belt in the India-Eurasia Collision: Evidence of SHRIMP II Zircon U-Pb Dating. *Acta Geol. Sinica*, 79(6): 787–794

Dong, G. C., Mo, X. X., Zhao, Z. D., et al., 2006. Magma Mixing in Middle Part of Gangdise Magma Belt: Evidences from Granitoid Complex. *Acta Petrologica Sinica*, 22(4): 835–844 (in Chinese with English Abstract)

Dong, G. C., Mo, X. X., Zhao, Z. D., et al., 2008. Gabbros from Southern Gangdese: Implication for Mass Exchange between Mantle and Crust. *Acta Petrologica Sinica*, 24(2): 203–210 (in Chinese with English Abstract)

Griffin, W. L., Wang, X., Jackson, S. E., et al., 2002. Zircon Chemistry and Magma Mixing, SE China: In-Situ Analysis of Hf Isotopes, Tonglu and Pingtan Igneous Complexes.

Lithos, 61(3–4): 237–269

Harris, N. B. W., Xu, R., Lewis, C. L., et al., 1988. Isotope Geochemistry of the 1985 Tibet Geotraverse, Lhasa to Golmud. *Phil. Trans. R. Soc. Lond.*, A327: 263–285

Hou, Z. Q., Gao, Y. F., Qu, X. M., et al., 2004. Origin of Adakitic Intrusives Generated during Mid-Miocene East-West Extension in Southern Tibet. *Earth Planet. Sci. Lett*., 220(1–2): 139–155

Ji, W. Q., Wu, F. Y., Chung, S. L., et al., 2009. Zircon U-Pb Geochronology and Hf Isotopic Constraints on Petrogenesis of the Gangdese Batholith, Southern Tibet. *Chemical Geology*, DOI: 10.1016/J.Chemgeo.2009.01.020

Jiang, W., Mo, X. X., Zhao, C. H., et al., 1999. Geochemistry of Granitoid and Its Mafic Microgranular Enclave in Gangdise Belt, Qinghai-Xizang Plateau. *Acta Petrol. Sinica*, 15(1): 89–97 (in Chinese with English Abstract)

Kemp, A. I. S., Hawkesworth, C. J., Foster, G. L., et al., 2007. Magmatic and Crustal Differentiation History of Granitic Rocks from Hf-O Isotopes in Zircon. *Science*, 315(5814): 980–983

Lee, H. Y., Chung, S. L., Wang, Y. B., et al., 2007. Age, Petrogenesis and Geological Significance of the Linzizong Volcanic Successions in the Linzhou Basin, Southern Tibet: Evidence from Zircon U-Pb Dates and Hf Isotopes. *Acta Petrol. Sinica*, 23(2): 493–500 (in Chinese with English Abstract)

Li, X. H., Li, Z. X., Li, W. X., et al., 2007. U-Pb Zircon, Geochemical and Sr-Nd-Hf Isotopic Constraints on Age and Origin of Jurassic I- and A-Type Granites from Central Guangdong, SE China: A Major Igneous Event in Response to Foundering of a Subducted Flat-Slab? *Lithos*, 96(1–2): 186–204

Mo, X. X., Dong, G. C., Zhao Z. D., et al., 2005a. Timing of Magma Mixing in Gangdise Magmatic Belt during the India-Asia Collision: Zircon SHIRMP U-Pb Dating. *Acta Geologica Sinica*, 79(1): 66–76

Mo, X. X., Dong, G. C., Zhao, Z. D., et al., 2005b. Spatial and Temporal Distribution and Characteristics of Granitoids in the Gangdese, Tibet and Implication for Crustal Growth and Evolution. *Geological Journal of China Universities*, 11(3): 281–290 (in Chinese with English Abstract).

Mo, X. X., Hou, Z. Q., Niu, Y. L., et al., 2007. Mantle Contributions to Crustal Thickening during Continental Collision: Evidence from Cenozoic Igneous Rocks in Southern Tibet. *Lithos*, 96(1–2): 225–242

Mo, X. X., Niu, Y. L., Dong, G. C., et al., 2008. Contribution of Syn-collisional Felsic Magmatism to Continental Crust Growth: A Case Study of the Paleogene Linzizong Volcanic Succession in Southern Tibet. *Chemical Geology*, 250: 49–67

Mo, X. X., Zhao, Z. D., Deng, J. F., et al., 2003. Response of Volcanism to the India-Asia Collision. *Earth Science Frontiers*, 10(3): 135–148 (in Chinese with English Abstract)

Ravikant, V., Wu, F. Y., Ji, W. Q., 2009. Zircon U-Pb and Hf Isotopic Constraints on Petrogenesis of the Cretaceous–Tertiary Granites in Eastern Karakoram and Ladakh, India. *Lithos*, DOI: 10.1016/J.Lithos.2008.12.013

Wen, D. R., Liu, D. Y., Chung, S. L., et al., 2008. Zircon SHRIMP U-Pb Ages of the Gangdese Batholith and Implications for Neo-Tethyan Subduction in Southern Tibet. *Chemical Geology*, 252(3–4): 191–201

Wu, F. Y., Yang, Y. H., Xie, L. W., et al., 2006. Hf Isotopic Compositions of the Standard Zircons and Baddeleyites Used in U-Pb Geochronology. *Chemical Geology*, 234(1–2): 105–126

Zhou, S., Mo, X. X., Dong, G. C., et al., 2004. ^{40}Ar-^{39}Ar Geochronology of Cenozoic Linzizong Volcanic Rocks in Linzhou Basin, Tibet, China, and Their Geological Implications. *Chinese Sci. Bull.*, 49: 1970–1979

Zhu, D. C., Mo, X. X., Zhao, Z. D., et al., 2009. Permian and Early Cretaceous Tectonomagmatism in Southern Tibet and Tethyan Evolution: New Perspective. *Earth Science Frontiers* (in Chinese with English Abstract) (in Press)